Cell Reports

Article

Involvement of a lateral entorhinal cortex engram in episodic-like memory recall

Graphical abstract

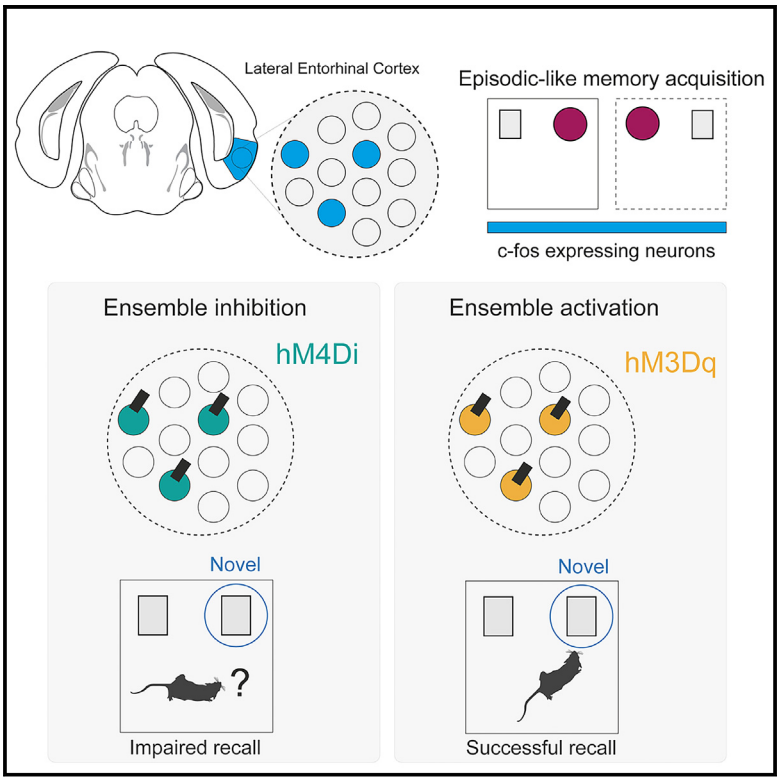

Authors

Francesca Tozzi, Stefano Guglielmo, Camilla Paraciani, Michel C. van den Oever, Marco Mainardi, Antonino Cattaneo, Nicola Origlia

Correspondence

origlia@in.cnr.it

In brief

Tozzi et al. demonstrate that the lateral entorhinal cortex (LEC) activation is crucial for episodic-like memory in mice. In particular, neuronal ensembles within the LEC allow the encoding and recall of object/place/context associations. The study emphasizes the role of this area in the broader network of episodic memory.

Highlights

- A specific LEC activation is induced by episodic-like memory processing
- Episodic-like memory expression correlates with LEC synaptic plasticity changes
- Inhibition of LEC learning-tagged neurons impairs episodic-like memory recall
- Reactivation of LEC engrams is crucial for episodic-like memory recall

Tozzi et al., 2024, Cell Reports *43*, 114795
October 22, 2024
https://doi.org/10.1016/j.celrep.2024.114795

CellPress

Cell Reports

CellPress
OPEN ACCESS

Article

Involvement of a lateral entorhinal cortex engram in episodic-like memory recall

Francesca Tozzi,[1,2] Stefano Guglielmo,[1,2] Camilla Paraciani,[2] Michel C. van den Oever,[3] Marco Mainardi,[2,4] Antonino Cattaneo,[1,5] and Nicola Origlia[2,6,*]

[1]BIO@SNS Laboratory, Scuola Normale Superiore, Via Moruzzi 1, 56124 Pisa, Italy
[2]Institute of Neuroscience, National Research Council, Via Moruzzi 1, 56124 Pisa, Italy
[3]Department of Molecular and Cellular Neurobiology, Center for Neurogenomics and Cognitive Research (CNCR), Amsterdam Neuroscience, Vrije Universiteit Amsterdam, De Boelelaan 1085, 1081 HV Amsterdam, the Netherlands
[4]Department of Biomedical Sciences University of Padova, 35122 Padova, Italy
[5]European Brain Research Institute Rita Levi-Montalcini, Via del Fosso di Fiorano 64/65, 00143 Rome, Italy
[6]Lead contact
*Correspondence: origlia@in.cnr.it
https://doi.org/10.1016/j.celrep.2024.114795

SUMMARY

Episodic memory relies on the entorhinal cortex (EC), a crucial hub connecting the hippocampus and sensory processing regions. This study investigates the role of the lateral EC (LEC) in episodic-like memory in mice. Here, we employ the object-place-context-recognition task (OPCRT), a behavioral test used to study episodic-like memory in rodents. Electrophysiology in brain slices reveals that OPCRT specifically induces a shift in the threshold for the induction of synaptic plasticity in LEC superficial layer II. Additionally, a dual viral system is used to express chemogenetic receptors coupled to the c-Fos promoter in neurons recruited during the learning. We demonstrate that the inhibition of LEC neurons impairs the performance of the mice in the memory task, while their stimulation significantly facilitates memory recall. Our findings provide evidence for an episodic-like memory engram in the LEC and emphasize its role in memory processing within the broader network of episodic memory.

INTRODUCTION

Episodic memory constitutes a crucial facet of long-term memory, facilitating individuals in the retrieval of personal experiences from their past. Investigating episodic memory in non-human animals, however, presents a significant challenge, especially in the absence of linguistic cues for conscious experiences.[1] To address this issue, Eacott and colleagues[2–4] developed a modified version of the spontaneous recognition paradigm known as the novel object-place-context recognition test (OPCRT) to evaluate animals' capability to recall the details of a past experience, including what happened, where it occurred, and under what circumstances. Notably, this behavioral assessment did not necessitate prior training, mirroring the nature of episodic memories as singular, one-time experiences. This paradigm uncovered the entorhinal cortex (EC) role in processing episodic-like memories in rodents.[5,6] Indeed, in both humans and non-human animals, episodic memory formation engages interconnected brain regions, in particular the hippocampus and parahippocampal areas,[7–11] and this anatomical and functional organization is highly conserved across mammalian species.[12] Recent research has provided insights into the specific involvement of the lateral entorhinal cortex (LEC) in encoding contextual information, which is essential for episodic memory. Numerous studies have demonstrated that the LEC performs associative learning upstream of the hippocampus, thereby providing a spatial framework for the creation of episodic memories.[13–17] Moreover, the LEC has been shown to play a fundamental role in encoding associations between objects, places, and contexts. Notably, Wilson et al.[18] demonstrated that the LEC is necessary for recognizing objects within a specific context, highlighting its involvement in object-context associations. The discovery of object trace cells in the rat EC by Tsao et al.[19] strengthened the hypothesis that the episodic memory system may operate similarly in animals and humans.[20] In addition, it has been demonstrated that lesions in the LEC impair odor-context associative memory in rodents, indicating that the EC, and in particular its lateral subdivision, plays a role in associative properties that extend beyond objects, places, and contexts, encompassing various features that constitute episodic memories.[21] Indeed, LEC neurons have been shown to possess the intrinsic ability to modulate their firing rates in a ramp-like fashion from the beginning of an event, enabling the encoding of the temporal context within an experience.[22–26]

Recently, the ability to target and study *in vivo* engram cells has allowed researchers to investigate the nature of the "enduring changes" induced by the memory process. Regarding contextual fear conditioning, studies have shown that the spines of CA1 engram cells receiving input from CA3

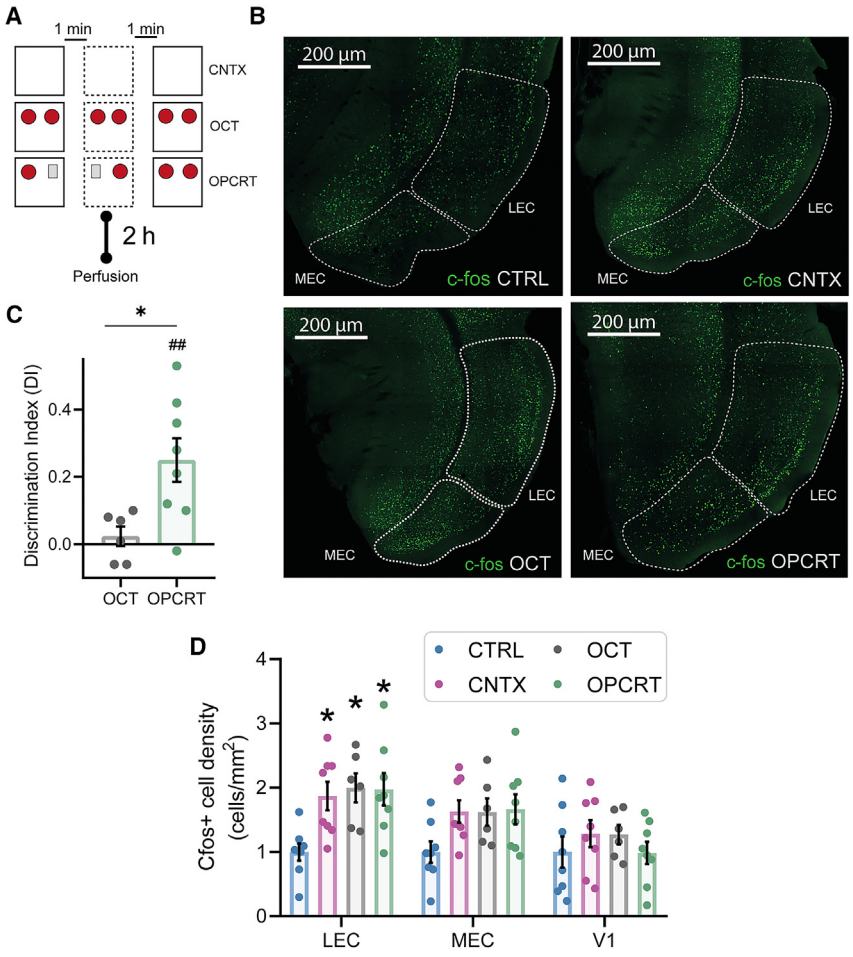

Figure 1. c-Fos cell density is increased in the LEC following OPCRT and context exploration

(A) Schematic representation of context exposure without objects (CNTX group), without novelty (exploration of two identical objects, OCT) and the OPCRT test, with animal perfusion that was performed 2 h after the behavioral task.

(B) Representative images displaying c-Fos expression (green) in the medial and LEC across various experimental groups.

(C) The discrimination index (DI) of mice subjected to OPCRT was significantly higher than chance (0.25 ± 0.06, n = 8, ##p = 0.0062, df = 7, t = 3.87, one-sample t test; $p < 0.01$), but no significant difference from chance level was observed for the OCT group (0.02 ± 0.03, n = 6, p = 0.46, df = 5, t = 0.80, one-sample t test). A significant difference was observed between the OCT and OPCRT group (0.02 ± 0.03, n = 6 OCT vs. 0.25 ± 0.06, n = 8 OPCRT, df = 12, t = 2.85, *p = 0.015 unpaired t test).

(D) A significant difference in c-Fos+ cell density was observed in the LEC (LEC) (two-way ANOVA with Tukey's multiple comparisons test: CTRL 1 ± 0.13 n = 8 vs. OPCRT 1.99 ± 0.22 n = 8, *p = 0.0127; CTRL vs. CNTX 1.87 ± 0.22 n = 8, *p = 0.0152; CTRL vs. OCT 1.97 ± 0.25 n = 6, *p = 0.0155). No significant difference was observed in the MEC (CTRL 1 ± 0.16 n = 8 mice vs. OPCRT 1.66 ± 0.23 n = 8 mice, p = 0.095; CTRL vs. CNTX 1.63 ± 0.2 n = 8 mice, p = 0.119; CTRL vs. OCT 1.62 ± 0.21, p = 0.177) and in the primary visual cortex (V1) (two-way ANOVA with Tukey's multiple comparisons test: CTRL 1 ± 0.24 n = 8 mice vs. OPCRT 0.985 ± 0.17 n = 8 mice, p = 0.99; CTRL vs. OCT 1.27 ± 0.15 n = 6 mice, p = 0.80; CTRL vs. CNTX 1.28 ± 0.21 n = 8 mice, p = 0.73). Values expressed as c-Fos+ cells/mm^2 relative to CTRL. Data are reported as mean ± SEM. Scale bar in (B), 20 µm.

engram cells increase in number and size, as demonstrated by Choi et al.[27] This enhanced connectivity between engram cells occludes long-term potentiation (LTP), confirming that a previous LTP-like phenomenon occurs during learning. Furthermore, there is growing evidence that engrams supporting specific episodic memories are widely distributed throughout the brain.[28] Nonetheless, concrete evidence supporting the participation of the LEC in the recall of episodic-like memory remains elusive. To address this question, we employed the protein encoded by the immediate-early gene (IEG) *c-Fos* as a marker of neuronal activity and observed its level in the EC after executing the OPCRT. Furthermore, we investigated whether changes in synaptic plasticity were specifically occurring in the LEC circuitry. Then, in order to trace and manipulate LEC neurons, we used a dual virus system, as previously established,[29] founded on the targeted recombination in active populations (TRAP) technology.[30] This allowed us to examine whether the activation of the LEC neuronal population involved during the learning phase of the paradigm was essential and adequate to demonstrate episodic-like OPCRT memory recall, thus indicating the existence of a memory engram within the LEC.

RESULTS

c-Fos-positive cell density is increased in the EC following OPCRT and context/object exploration

To investigate whether the processing of an episodic-like memory engages the EC and triggers the expression of plasticity-related genes, the number of cells that are positive for the IEG-encoded c-Fos protein was assessed 2 h after the execution of the behavioral task (Figure 1A).

The results showed that the mice in the OPCRT group exhibited a significant preference for the novel object-place-context configuration compared to the familiar one, indicating the presence of episodic-like memory (Figure 1C). A significant preference for one object was not observed in the behavioral control that excluded the novelty, in which mice were subjected to the two copies of the object across two contexts (as in the test trial) and then tested on context A (OCT group; Figures 1A and 1C). The processing of the OPCRT memory was associated with a significant increase in c-Fos-positive cell density in the LEC subdivision compared to control (CTRL) mice (Figures 1B and D), suggesting that this region was strongly recruited during the task. A similar increase was observed in the LEC of OCT mice

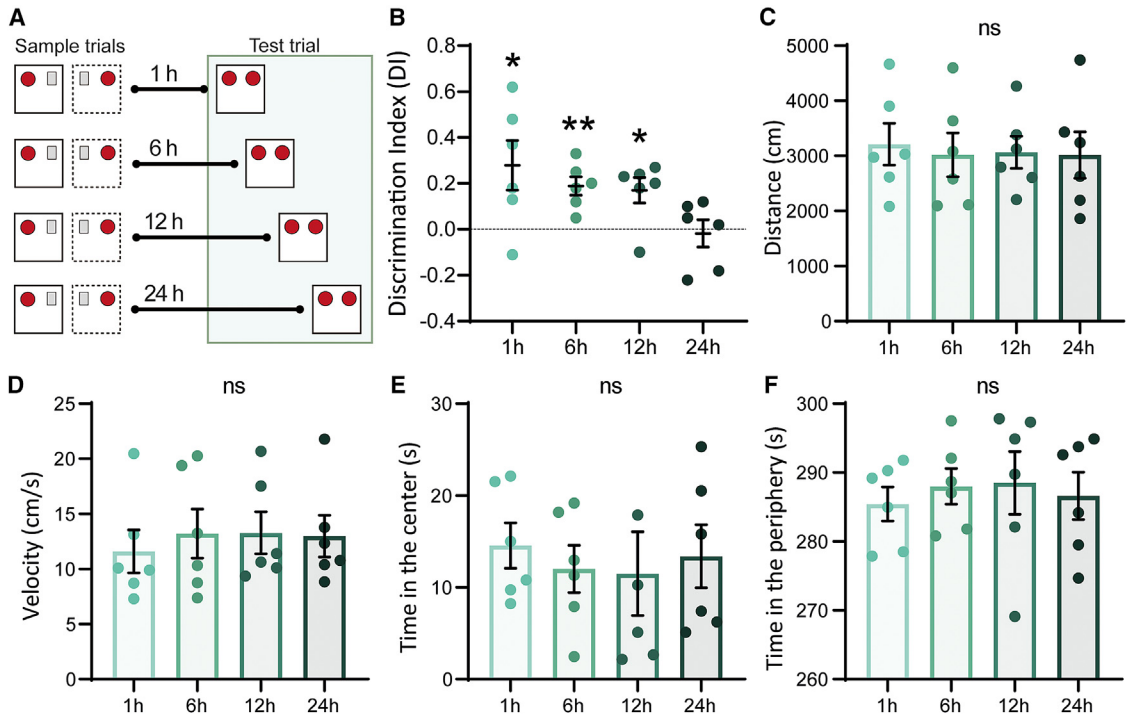

Figure 2. Time course of object-place-context recognition memory

(A) Schematic representation of the delayed OPCRT test, with the test trial conducted at different time intervals (1, 6, 12, or 24 h) following the sample trial presentation.

(B) The DIs for the novel OPC association exhibits a significant decline with increasing time intervals from the sample trials presentation ($p = 0.037$, Kruskal-Wallis test). Mice were able to recall the previously acquired episodic-like memory at either 1 h (0.28 ± 0.11, $n = 6$, $p = 0.049$, df = 5, t = 2.58), 6 h (0.19 ± 0.04, $n = 6$, $p = 0.0053$, df = 5, t = 4.71) ,or 12 h (0.17 ± 0.06, $n = 6$, $p = 0.03$, df = 5, t = 3.06; one-sample t test), while no memory was observed at 24 h (-0.018 ± 0.06, $n = 6$, $p = 0.77$, df = 5, t = 0.31, one-sample t test).

(C) No significant difference in the total distance traveled during the open field test was observed between experimental groups ($n = 6$, $p = 0.97$, F = 0.06, one-way ANOVA).

(D) The animal velocity during the open field test did not differ significantly among groups ($n = 6$, $p = 0.92$, F = 0.16 one-way ANOVA).

(E) The time spent in the center of the arena by the animals was similar among the different experimental groups ($n = 6$, $p = 0.92$, f = 0.17, one-way ANOVA).

(F) The animals spent a comparable amount of time in the arena's periphery ($n = 6$, $p = 0.92$, f = 0.17, one-way ANOVA). $^*p < 0.05$, $^{**}p < 0.01$. Data are reported as mean ± SEM.

(Figures 1B and 1D). However, c-Fos staining increased significantly also in the context (CNTX) group, indicating that the presence of objects is not necessary to engage this circuitry (Figures 1B and 1D).

Interestingly, no significant increase in c-Fos-positive cell density was observed in the same conditions either in the medial entorhinal cortex (MEC) or in another cortical area, the primary visual cortex (V1) (Figure 1D). Nevertheless, it is worth noting that, while no specific trend was observed in V1, the MEC displayed a tendency toward increased c-Fos levels in the CNTX, OCT, and OPCRT groups, indicating that this region might be slightly affected by episodic-like memory processing as well.

In order to investigate whether episodic-like memory could affect not only the number of c-Fos-positive cells but also the relative amount of c-Fos protein produced by individual EC cells, the mean fluorescence intensity of single cells per animal was examined in the same experimental groups. However, no significant difference in c-Fos fluorescence intensity was found in the areas of interest (Figure S1). These results suggest that the recruitment of a large group of LEC neurons, as assessed by c-Fos staining, is induced by the processing of episodic-like memory, but this phenomenon does not lead to changes in the amount of c-Fos protein produced by each individual cell. To verify whether the observed effects were not due to behavioral differences in exploratory behavior between the OPCRT, OCT, and CNTX groups, an open field test was performed before the experiments and the time spent in the center vs. periphery of the arena, the average velocity, and the traveled distance were analyzed (Figure S1). Moreover, exploratory behavior during the test trial did not significantly change between groups (Figure S1).

Time course of object-place-context recognition memory

In order to characterize the time course of object-place-context recognition memory, a delayed OPCRT was performed during which the test trial presentation was delayed by 1, 6, 12, or 24 h after the sample trials (Figure 2A). Different groups of animals were utilized at each time point to prevent potential effects on memory recall from repeatedly administering test trials to the

same animal. By analyzing changes in the discrimination index over these time points, the temporal expression of episodic-like memory could be estimated, allowing for the identification of the time window during which the memory was behaviorally expressed. Results showed a significant preference for the novel object-place-context (OPC) association within the first 12 h following the sample trials, indicating effective recall of the previously acquired memory. However, after 24 h, novelty discrimination significantly declined (Figure 2B).

It is worth noting that the observed differences in memory expression were not attributed to differences in anxiety levels or exploratory behavior as there was no significant difference in the traveled distance (Figure 2C), the average velocity (Figure 2D), and the time spent in the center/periphery of the arena (Figures 2E and 2F) among the groups.

OPCRT induces changes in LTP and LTD expression in the LEC intrinsic circuitry

Memory acquisition has been shown to trigger persistent changes in synaptic efficacy, indicating the involvement of synaptic plasticity in memory storage.[31] To investigate whether processing of episodic-like memory can affect synaptic plasticity in the LEC, field excitatory postsynaptic potentials (fEPSPs) were recorded in EC slices obtained from mice subjected to OPCRT and sacrificed 12 h later. Specifically, it was assessed whether any alterations in long-lasting forms of plasticity, such as LTP and long-term depression (LTD), were present at a time point when memory was still behaviorally expressed, thus exploring the possible association between long-lasting plasticity and memory expression (Figure 3A).

Indeed, a significant leftward shift in the input/output (I/O) curve was observed in the LEC in the OPCRT group compared to the CNTX and CTRL groups, which could reflect an increased excitatory transmission in the horizontal connections of the LEC following memory acquisition (Figure 3B). When high-frequency stimulation (HFS) was applied to LEC superficial layer, a significant reduction in LTP was observed in slices from OPCRT mice compared to CNTX or CTRL groups, suggesting that the processing of an episodic memory had already potentiated synaptic transmission in the LEC superficial layers (Figure 3C). This effect was OPCRT specific since context exploration was not sufficient to induce such changes in synaptic efficacy. Moreover, slices from OPCRT mice showed enhanced low-frequency stimulation (LFS)-induced LTD compared to CNTX and CTRL groups (Figure 3D), confirming that the processing of a new episodic-like memory might specifically induce a shift in the threshold for the induction of synaptic plasticity moving synaptic efficacy toward higher values.

It is worth noting that no significant changes either in HFS- or LFS-induced synaptic plasticity were observed in the superficial layers of the MEC 12 h following the execution of the task, suggesting that OPCRT did not affect synaptic plasticity in MEC circuitry or that the changes were not detectable as assessed by fEPSP recordings (Figures 3E and 3F).

Long-term plasticity is considered the basis of learning and memory and represents a physiological phenomenon enabling the storage of information for long periods of time. We hypothesized that, if the plasticity effects observed following OPCRT played a role in retaining information about a previous episode, they should return to baseline when the memory was not behaviorally expressed anymore. To test this, the electrophysiological experiments were repeated 48 h following the execution of the task (Figure S2). At this time point, LEC slices showed normal synaptic transmission when compared to controls. Indeed, the HFS-induced LTP and LFS-induced LTD in LECs slices at 48 h were comparable to that of CTRL, indicating that the episodic-like memory-induced changes in LEC synaptic transmission were indeed reversible.

The detection and the time course of specific synaptic plasticity changes in the LEC prompted us to further investigate the existence of an OPCRT memory trace in this area.

The activation of LEC learning-tagged neurons is necessary for episodic-like but not for non-associative memory recall

Based on previous results, it could be hypothesized that the LEC neurons may retain information from past experiences, which could be accessed during memory recall. To validate this hypothesis, a double virus system, previously developed,[29] was used, based on the TRAP technology.[30] This method allowed us to target the LEC neurons recruited during the learning phase of the paradigm and manipulate their activity during memory recall. Specifically, an adeno-associated virus (AAV) coding for the inducible Cre recombinase under the control of the c-Fos promoter (AAV-Fos::CreERT2) and Cre-dependent AAV containing the coding sequence of the inhibitory chemogenetic receptor hM4Di in an inverse open reading frame flanked by Cre recognition sites were injected bilaterally in the LEC of 2-month old C57BL6 mice. Then, by administering 4-hydroxytamoxifen (4OH-TAM intraperitoneally [i.p.]) 4 h before the presentation of the OPCRT sample trials, the expression of the chemogenetic receptor was induced in the learning-tagged neurons specifically in the LEC (Figure 4A). A control group receiving a Cre-dependent mCherry reporter without hM4Di was included for comparison (mCherry mice; Figures 4C and 4E–4G). Initially, the ability of 4OH-TAM administration to induce the expression of the chemogenetic receptor was verified by analyzing the density of mCherry-positive cells after the OPCRT in mice that were injected with 4OH-TAM compared to those injected with the vehicle. Results indicated that mice that received a Cre-dependent mCherry reporter with hM4Di and injected with 4OH-TAM showed a significantly higher number of mCherry-positive cells 16 h post treatment compared to those that were injected with the same viral system but received the vehicle (Figures 4B and 4D). Indeed, whole-cell patch-clamp recordings of superficial layer neurons in LEC slices from mice that received a Cre-dependent mCherry reporter without hM4Di revealed that OPCRT significantly increased spontaneous excitatory postsynaptic currents (EPSCs) in learning-tagged neurons (mCherry positive) but not in neurons that do not express the fluorescent reporter (mCherry negative; see Figure S3). This is in agreement with the LTP results of Figure 3 and confirms an increase in the synaptic strength that is specifically associated with the behavioral task.

Next, it was investigated whether the activation of learning-tagged LEC neurons was crucial for achieving a successful

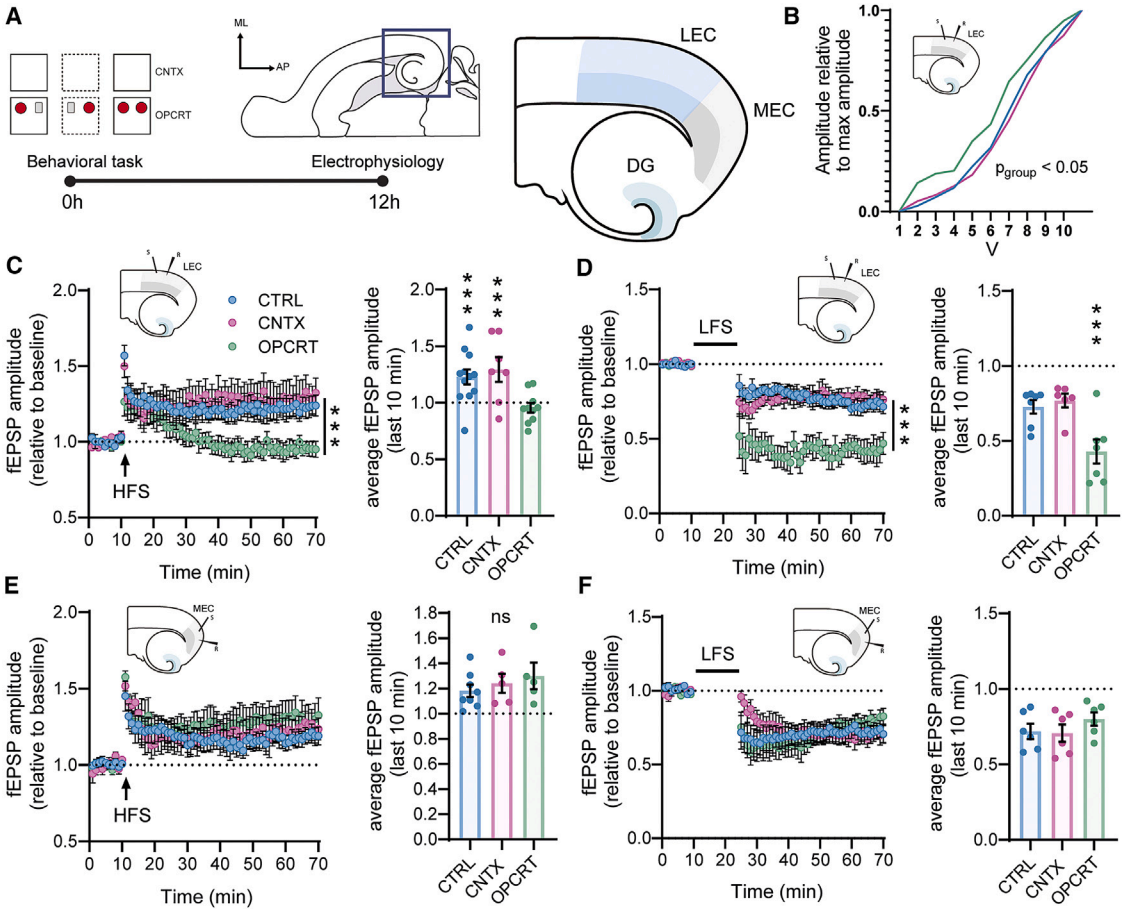

Figure 3. OPCRT-induced long-term changes in LEC synaptic plasticity

(A) Timeline of the experimental design and plane of EC slice sectioning.

(B) The input/output (I/O) relationship in slices obtained from OPCRT mice was significantly rightward shifted compared to slices obtained from either CNTX or CTRL mice (p(group effect) = 0.037, df = 2, F = 3.62 two-way ANOVA RM).

(C) (Left) Time course of field excitatory postsynaptic potentials (fEPSPs) during the LTP protocol. (Right) The average fEPSPs on the last 10 min of recordings. Slices obtained from either CNTX or CTRL mice showed high-frequency stimulation (HFS)-induced long-term potentiation (LTP) 12 h after the execution of the behavioral tasks (p(interaction) = 0.007, p(time) = 0.001, p(group) = 0.0066 two-way ANOVA RM; 129% ± 11% of baseline, n = 7 slices [four mice], p = 0.005 vs. baseline for CNTX; 123% ± 7% of baseline, n = 12 slices [five mice], p = 0.0043 vs. baseline for CTRL, Sidak's multiple comparisons test), while no significant LTP was observed in OPCRT slices (95% ± 4% of baseline, n = 10 slices [five mice], p = 0.89, two-way ANOVA RM and Sidak's multiple comparisons test). OPCRT slices were significantly different when compared to CTRL (95% ± 4% of baseline, n = 10 slices [five mice] OPCRT vs. 123% ± 7% of baseline, n = 12 slices [five mice] CTRL, p = 0.0005) or CNTX slices (95% ± 4% of baseline, n = 10 slices [five mice] OPCRT vs. 129% ± 11% of baseline, n = 7 slices [four mice] CNTX, p = 0.0002, two-way ANOVA RM and Sidak's multiple comparisons test).

(D) Same as in (C) but for the LTD protocol. Significant levels of low-frequency stimulation (LFS)-induced LTD were observed in all the groups in the LEC 12 h after the execution of the behavioral tasks (73% ± 4% of baseline, n = 7 slices [four mice], p = 0.0007 vs. baseline for CTRL; 77% ± 5% of baseline, n = 6 slices [three mice], p = 0.0063 vs. baseline for CNTX; 43% ± 8% of baseline, n = 7 slices [four mice], p < 0.0001 vs. baseline for OPCRT; two-way ANOVA RM and Sidak's multiple comparisons test). However, in OPCRT slices, LTD in the LEC was significantly enhanced compared either to CTRL (43% ± 8% of baseline, n = 7 slices [four mice] OPCRT vs. 73% ± 4% of baseline, n = 7 slices [four mice] CTRL, p < 0.001) or CNTX (43% ± 8% of baseline, n = 7 slices [four mice] OPCRT vs. 77% ± 5% of baseline, n = 6 slices [three mice] CNTX, p < 0.001, two-way ANOVA RM and Sidak's multiple comparisons test).

(E) Same as in (C) but for the medial EC (MEC). In the MEC, a significant LTP was observed in all the groups following HFS (118% ± 5% of baseline, n = 8 slices [four mice], p = 0.034 vs. baseline for CTRL; 124% ± 8% of baseline, n = 5 slices [three mice], p = 0.026 vs. baseline for CNTX; 130% ± 11% of baseline, n = 5 slices [three mice], p = 0.0057 vs. baseline for OPCRT; two-way ANOVA RM and Sidak's multiple comparisons tests), with no significant difference between the experimental groups observed 12 h following the execution of the behavioral tasks in the superficial layers (p(group effect) = 0.52, df = 2, F = 0.69, two-way ANOVA RM).

(F) Same as in (E) but for the LTD protocol. A significant LTD was observed in the MEC in all the groups following LFS (72% ± 5% of baseline, n = 6 slices [three mice], p = 0.0002 vs. baseline for CTRL; 71% ± 6% of baseline, n = 6 slices [three mice], p = 0.0001 vs. baseline for CNTX; 80% ± 4% of baseline, n = 6 slices [three mice], p = 0.004 vs. baseline for OPCRT). However, no significant difference between groups was observed (p(group effect) = 0.39, df = 2, F = 0.99 two-way ANOVA RM). ***p < 0.001. The inserts show the positioning of the stimulating electrode (s) and recording pipette (r). DG, dentate gyrus. Data are reported as mean ± SEM.

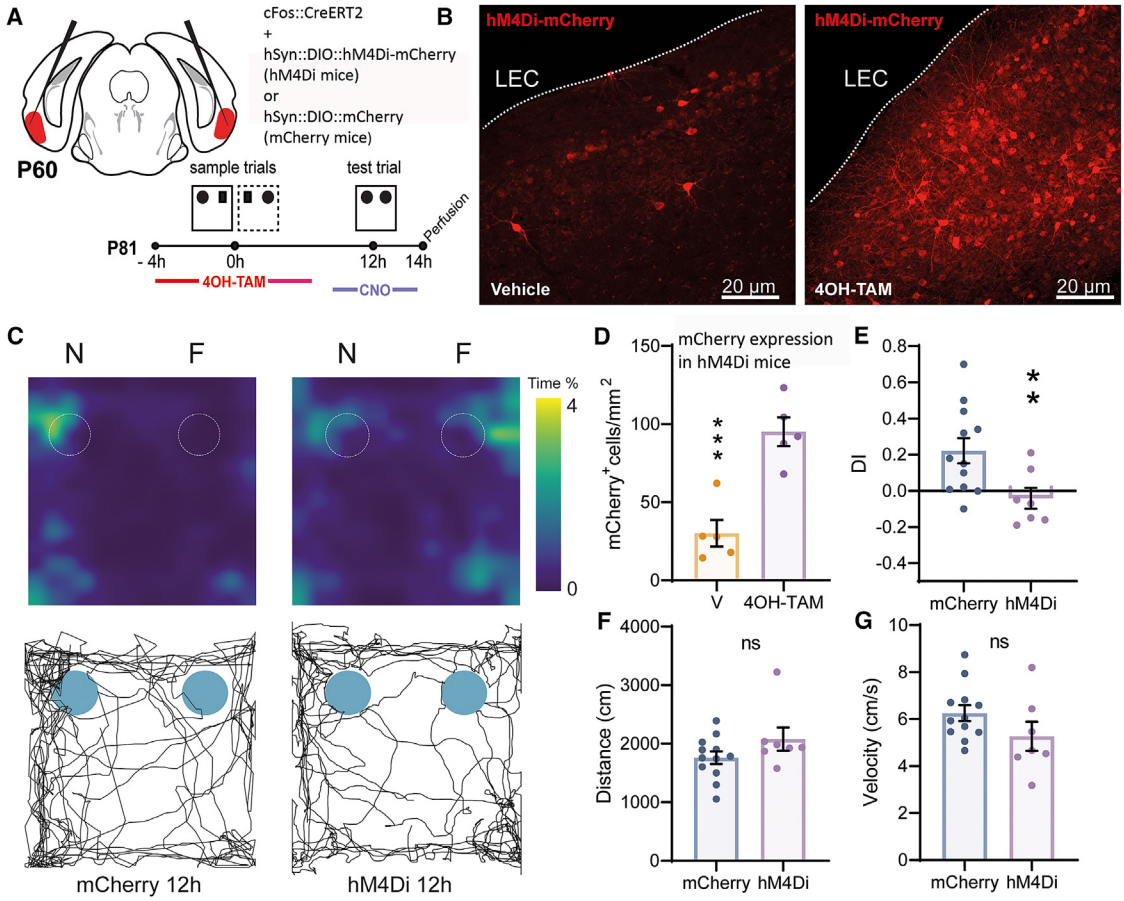

Figure 4. Chemogenetic inhibition of LEC learning-tagged neurons

(A) Experimental timeline showing the injection of two AAV5 viral constructs, cFos::CreERT2 and hSyn::DIO::hM4Di-mCherry, at p60 and the OPCRT memory paradigm at p81. Four hours before the execution of the sample trials, mice received an i.p. injection of 4OH-TAM (25 mg/kg) to induce the recombination and expression of the inhibitory chemogenetic receptor; 30 min before the execution of the test trial, they received an i.p. injection of CNO to induce the activation of the hM4Di receptor.

(B) Representative images showing the expression of hM4Di-mCherry either in mice injected with the vehicle or mice injected with 4OH-TAM at the following coordinates: ML = −3.9, AP = −3, and DV = 4.5 from Bregma.

(C) Examples of heatmaps and tracking plots of the exploratory activity of mice (position of the nose) during the test trial of the OPCRT paradigm.

(D) The density of hM4Di-expressing neurons was significantly higher in mice injected with 4OH-TAM compared to mice injected with the vehicle (95.15 ± 9 cells/mm^2, n = 5 4OH-TAM vs. 30.16 ± 8 cells/mm^2 vehicle, p = 0.0008, df = 5, t = 5.2, two-tailed unpaired t test).

(E) The DIs of mCherry mice 12 h following the presentation of the sample trials was significantly higher than chance (0.22 ± 0.07, n = 12, p = 0.0087, df = 11, t = 3, one-sample t test). In contrast, the DI of hM4Di mice did not differ from chance levels (−0.04 ± 0.06, n = 7, p = 0.50). Moreover, the two groups were significantly different from each other (mCherry 12 h vs. hM4Di, p = 0.02, df = 17, t = 2.6, two-tailed unpaired t test).

(F) No significant difference in the distance traveled during the test trial between groups (1,761 ± 106 cm, n = 12 mCherry vs. 2,079 ± 199 cm, n = 7 hM4Di, p = 0.14, df = 17, t = 1.53, two-tailed unpaired t test).

(G) No significant difference in average velocity between groups during the test trial (6.26 ± 0.34 cm/s, n = 12 mCherry vs. 5.1 ± 0.56 cm/s, n = 8 hM4Di, p = 0.08, two-tailed unpaired t test). **p < 0.01, ***p < 0.001. Scale bar in (B), 20 µm. Data are reported as mean ± SEM.

memory recall. Notably, pharmacological inhibition of LEC neurons by clozapine-N-oxide (CNO) administration significantly impaired the ability to discriminate novel OPC associations in the hM4Di-expressing group 12 h after the sample trials, whereas CNO had no effect in mice expressing the mCherry reporter alone (mCherry group), which displayed normal episodic-like memory (Figures 4E and 4C).

To exclude the possibility that the observed behavioral effect was caused by differences in exploratory activity or anxiety levels, the average velocity and total distance traveled during the test trial were measured either in hM4Di and mCherry mice, but no significant differences were found (Figures 4C, 4F, and 4G). As an additional control, an open field test was performed immediately before the execution of the OPCRT and demonstrated that both groups had comparable exploratory activity (Figure S4), supporting the hypothesis that the disruption in memory recall was the result of the inhibition of a specific neuronal ensemble in the LEC. In order to determine whether the impairment of episodic-like memory recall caused by the inhibition of LEC neurons was due to impaired detection of novelty

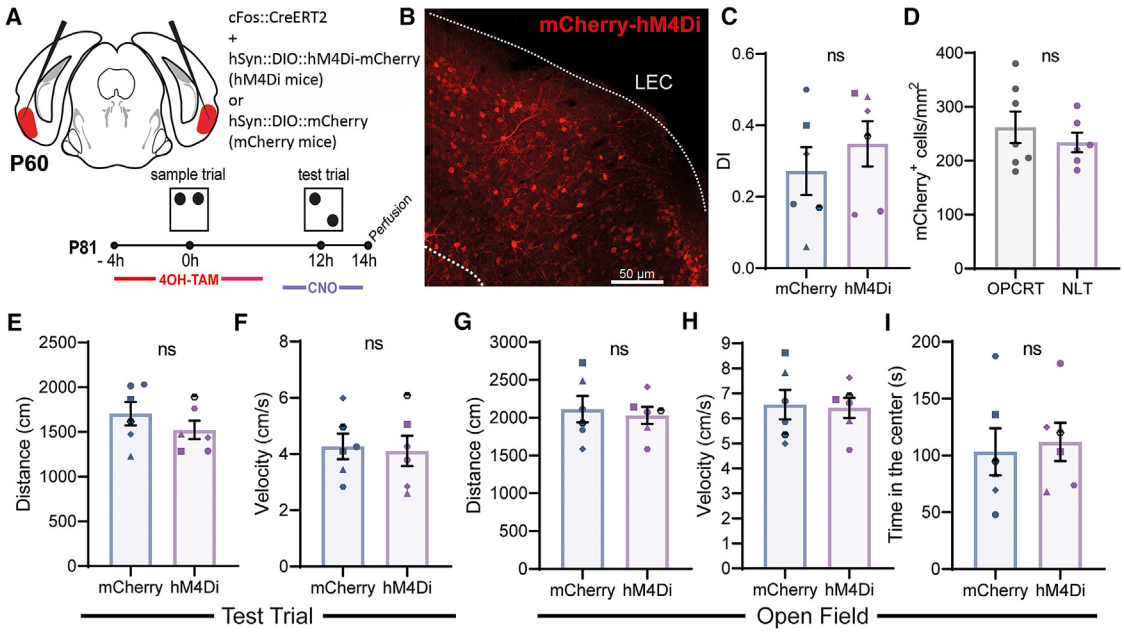

Figure 5. Inhibition of LEC learning-tagged neurons does not affect non-associative memory recall

(A) Experimental timeline showing the injection of two AAV5 viral constructs, cFos::CreERT2 and hSyn::DIO::hMDDi-mCherry, at p60 and the novel location test (NLT) memory paradigm at p81. Four hours before the execution of the sample trials, mice received an i.p. injection of 4OH-TAM to induce the recombination and expression of the inhibitory chemogenetic receptor; 30 min before the execution of the test trial, they received an i.p. injection of CNO to induce the activation of the hM4Di receptor.

(B) Representative image showing the expression of hM4Di-mCherry in the LEC of mice after 4OH-TAM administration at the following coordinates: ML = −3.9, AP = −3, and DV = 4.5 from Bregma.

(C) Mice in the mCherry (0.27 ± 0.07, $n = 6$ vs. chance level, $p = 0.01$, df = 5, t = 4.06 one-sample t test) and hM4Di (0.35 ± 0.06, $n = 6$ vs. chance level, $p = 0.003$, df = 5, t = 5.48 one-sample t test) showed significant memory for the familiar location. No difference was observed between the two experimental groups (two-tailed unpaired t test).

(D) In the LEC, no difference was observed in the number of learning-tagged neurons (mCherry+) between mice that performed the OPCRT and those that were tested in the NLT (262 ± 36 mCherry+/mm^2, $n = 7$ vs. 234 ± 26 c-Fos + mCherry+/mm^2, $n = 6$, $p = 0.45$, df = 11, t = 0.77 two-tailed unpaired t test).

(E) Mice in the mCherry and hM4Di groups did not differ in the distance traveled during the test trial (1,705 ± 131 cm, $n = 6$ mCherry vs. 1,523 ± 102 cm, $n = 6$ hM4Di, $p = 0.30$, df = 10, t = 1.093, two-tailed unpaired t test).

(F) No difference in the animal velocity during the test trial (4.27 ± 0.45 cm/s, $n = 6$ mCherry vs. 4.11 ± 0.54 cm/s, $n = 6$ hM4Di, $p = 0.83$, df = 10, t = 0.23, two-tailed unpaired t test).

(G) Mice showed similar distance traveled during the open field test (2,114 ± 174 cm, $n = 6$ mCherry vs. 2,029 ± 1,103 cm, $n = 6$ hM4Di, $p = 0.69$, df = 10, t = 0.41, two-tailed unpaired t test).

(H) No difference was observed in the animal velocity during the open field test (6.56 ± 0.59 cm/s, $n = 6$ mCherry vs. 6.43 ± 0.41 cm/s, $n = 6$ hM4Di, $p = 0.86$, df = 10, t = 0.18, two-tailed unpaired t test).

(I) Mice showed no significant difference in the time spent in the center of the arena during the open field test (103.3 ± 20.7 s, $n = 6$ mCherry vs. 111.9 ± 16.8 s, $n = 6$ hM4Di, $p = 0.75$, df = 10, t = 0.32, two-tailed unpaired t test). In the plots each symbol identifies an individual animal. Scale bar in (B), 50 μm. Data are reported as mean ± SEM.

in individual components of the task, a follow-up experiment was conducted using a non-associative task called the novel location test (NLT; Figures 5A and 5B). This task did not require the learning of an association between stimuli, but, rather, the novelty was represented by a different location within a familiar context. As reported in Figure 5, chemogenetic inhibition of learning-tagged LEC neurons did not affect the ability to recognize the novel location compared to the familiar one. A control group receiving a Cre-dependent mCherry reporter without hM4Di was included for comparison (mCherry mice; Figures 5C and 5E–5I), but no significant difference was observed after CNO administration between the hM4Di and mCherry groups (Figure 5C) and in the LEC the number of NLT learning-tagged cells was comparable to that induced by the OPCRT(Figure 5D). The exploratory behavior during the test trial was similar between the experimental groups (Figures 5E and 5F) and mice did not show any behavioral impairment in an open field test (Figures 5G, 5H, and 5I), indicating that the observed differences in episodic-like memory recall were not due to different exploration of the environment or increased anxiety.

Together, these results suggest that the activation of learning-tagged LEC neurons is specifically required for the recall of associative episodic-like memory and not for non-associative behavioral tasks, indeed not affecting the ability of the mice to discriminate novelty or remember the individual non-associative components of the behavior, such as the memory for spatial location.

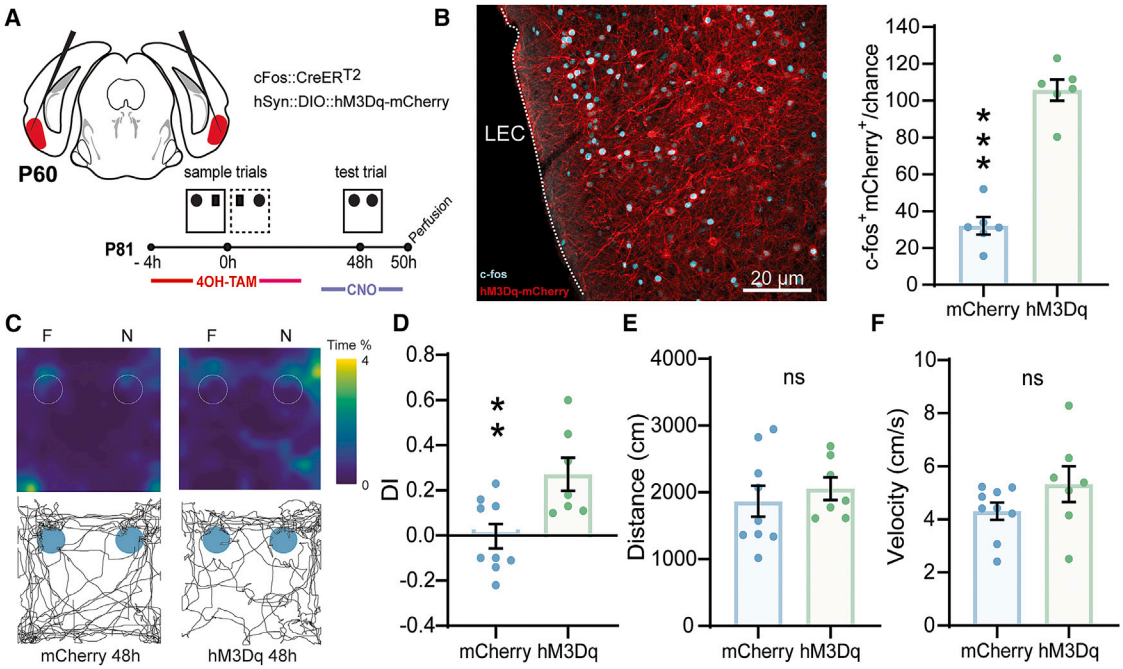

Figure 6. The activation of LEC neurons facilitates episodic-like memory recall

(A) Experimental timeline showing the injection of two AAV5 viral constructs, cFos::CreERT2 and hSyn::DIO::hMDDi-mCherry, at p60 and the OPCRT memory paradigm at p81. Four hours before the execution of the sample trials, mice received an i.p. injection of 4OH-TAM to induce the recombination and expression of the inhibitory chemogenetic receptor; 30 min before the execution of the test trial, they received an i.p. injection of CNO to induce the activation of the hM3Dq receptor.

(B) The overlap of mCherry- and c-Fos-expressing neurons over chance levels was significantly higher in the hM3Dq group compared to the mCherry one (31.98 ± 4.8 c-Fos+ mCherry+/chance levels, $n = 6$ mCherry vs. 105.7 ± 5.8 c-Fos + mCherry+/chance levels, $n = 6$ hM3Dq, $p < 0.001$, df = 10, t = 9.9 two-tailed unpaired t test). Representative image acquired at the following coordinates: ML = −3.9, AP = −3, and DV = 4.5 from Bregma.

(C) The figures present heatmaps and tracking plots that depict the exploratory activity of mice during the test trial of the OPCRT paradigm. The tracking plots illustrate the trajectory of the mouse's nose.

(D) Mice expressing the control reporter mCherry did not remember the previously acquired OPC association 48 h following learning (−0.003 ± 0.05, $n = 9$ vs. chance level, $p = 0.95$, df = 8, t = 0.06), while hM3Dq mice showed a strong preference for the novel association (0.27 ± 0.07, $n = 7$ vs. chance level, $p = 0.01$, df = 6, t = 3.7, one-sample t test). Indeed, the DI of mCherry mice was significantly lower than the DI of hM3Dq animals (−0.003 ± 0.05, $n = 9$ mCherry vs. 0.27 ± 0.07, $n = 7$, $p = 0.008$, df = 14, t = 3.1, two-tailed unpaired t test).

(E) The total distance traveled during the test trial was not different between the mCherry and hM3Dq groups (1,866 ± 232.1 cm, $n = 9$ mCherry vs. 2,054 ± 169.2 cm, $n = 7$ hM3Dq, $p = 0.54$, df = 14, t = 0.62, two-tailed unpaired t test).

(F) The average velocity was comparable among groups (4.32 ± 0.32 cm/s, $n = 9$ mCherry vs. 5.33 ± 0.68 cm/s, $n = 7$ hM3Dq, $p = 0.17$, df = 14, t = 1.5, two-tailed unpaired t test). $^{**}p < 0.01$, $^{***}p < 0.001$. Scale bar in (B), 20 μm. Data are reported as mean ± SEM.

The activation of LEC learning-tagged neurons facilitates episodic-like memory recall

To investigate whether activation of the LEC learning-tagged neurons was also sufficient to facilitate memory recall, chemogenetic stimulation of these neurons was conducted using the expression of excitatory chemogenetic receptor hM3Dq.

Prior to sample trials, mice were injected with 4OH-TAM to tag the LEC neurons expressing c-Fos during learning, which were then artificially reactivated 48 h later during the test trial by the administration of CNO (Figure 6A). To verify the efficacy of hM3Dq receptors in activating LEC neurons, we conducted immunofluorescence against c-Fos at 2 h following the manipulation of neurons on a subset of experimental animals. The results showed a significant increase in the overlap of mCherry+/c-Fos+ cells in hM3Dq-expressing mice compared to mice expressing mCherry alone, indicating efficient activation of LEC-tagged neurons (Figure 6B). In the mCherry control group, the overlap was also higher than chance, which implies that even in the absence of chemogenetic manipulation, a subset of the original neuronal ensemble was still reactivated when the animal re-encountered the familiar object/place/context association.

At the behavioral level, control mice injected with mCherry reporter alone did not exhibit episodic-like memory 48 h after the execution of sample trials, in agreement with the physiological memory time course reported in Figure 2. However, at this time point and after CNO administration, hM3Dq-expressing mice showed a significant preference for the novel OPC association (Figures 6C and 6D) with respect to mice expressing mCherry alone. The differences observed in control mice were not due to a different exploratory behavior as mCherry and hM3Dq mice showed comparable velocity and traveled distance during the test trial (Figures 6C, 6E, and 6F). No changes in open field behavior were also observed (Figure S5). These data indicate that the stimulation of LEC learning-tagged neurons alone

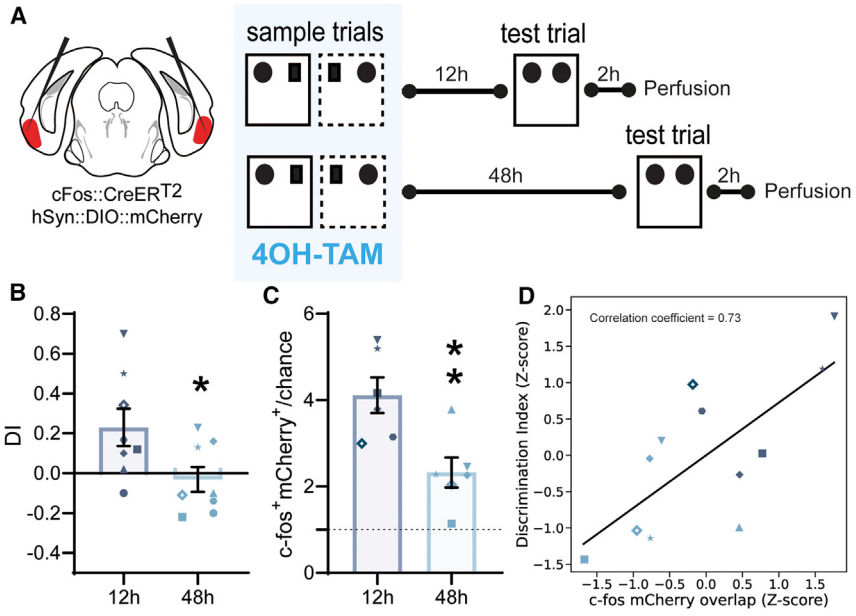

Figure 7. Reactivation of learning-tagged neurons by natural recall cues

(A) Timeline of the experimental design.

(B) Mice expressing the reporter mCherry were able to recall the previously acquired episodic-like memory when the test trial was presented 12 h following learning (0.23 ± 0.10, $n = 8$, $p = 0.04$, df = 7, t = 2.4, one-sample t test) but not when the test trial was performed 48 h after learning (−0.03 ± 0.06, $n = 8$, $p = 0.63$, df = 7, t = 0.5, one-sample t test). The discrimination indices of the two groups were significantly different (mCherry 12h vs. mCherry 48 h, $p = 0.04$, df = 14, t = 2–3, two-tailed unpaired t test).

(C) The reactivation of the LEC learning-tagged neurons, measured as the percentage of c-fos+mCherry+ overlap over chance levels, was higher in mCherry mice exposed to the test trial at 12 h with respect to mice exposed to the test trial at 48 h (4.11 ± 0.41, $n = 6$ mCherry 12 h vs. 2.33 ± 0.35, $n = 6$ mCherry 48 h, $p = 0.008$, df = 10, t = 3.3, two-tailed unpaired t test). However, both at 12 and 48 h, the reactivation was significantly different from chance levels (4.11 ± 0.41, $n = 6$ mCherry 12 h vs. chance, $p = 0.0006$; 2.33 ± 0.35, $n = 6$ mCherry 48 h, $p = 0.013$, one-sample t test); in the plots each symbol identifies an individual animal.

(D) A significant correlation was observed between the percentage of c-Fos/mCherry overlap and the DIs (Pearson correlation, $p = 0.008$, correlation coefficient = 0.73). Data are reported as mean ± SEM.

is not only necessary but also sufficient to facilitate memory recall, thus strengthening the hypothesis that key information about previous episodes might be retained in LEC neuronal ensembles and that their reactivation might be necessary to access the stored information.

LEC learning-tagged neurons are reactivated by natural recall cues

If the activation of a specific neuronal ensemble is necessary and sufficient for memory recall, as for the definition of a neuronal engram, the same neuronal ensemble should be more likely to be reactivated when the animal expresses the memory behaviorally compared to those situations where the animal fails to retrieve the previous experience. To confirm this hypothesis for LEC neurons, we measured the overlap between mCherry and c-Fos expression in control mice injected with Cre-dependent mCherry reporter and subjected to memory recall either 12 h (mCherry 12-h group) or 48 h (mCherry 48-h group) after the sample trials presentation (Figure 7A). As expected, we found that mCherry mice significantly discriminated between the new and the familiar OPC associations at 12 h, while failing to do so at 48 h (Figure 7B).

The immunofluorescence analysis revealed that the overlap between mCherry and c-Fos was significantly higher in the mCherry group at 12 h compared to the mCherry at 48 h and significantly correlated with the discrimination index (DI), supporting the hypothesis that the reactivation of LEC neurons induced by natural recall cues may represent the physiological process through which successful recall is achieved (Figures 7C and 7D).

These findings corroborate the association between LEC neuronal ensemble activation and episodic-like memory recall, thus reinforcing the idea that essential information regarding past experiences is encoded within this network and is utilized to accomplish effective memory recall.

DISCUSSION

The EC is a crucial link between the hippocampus and multisensory cortical areas. It consists of two subdivisions, the lateral and medial EC, which have been traditionally associated with conveying contextual and spatial information, respectively, to the hippocampus for the integration of memories.[17,32,33] However, emerging evidence suggests that this conceptualization of parallel information streams in the EC may be oversimplified as confirmed by analysis of projection patterns into the EC.[34,35] Indeed, the EC itself may play a direct role in integrating different types of information into a cohesive experience even before they reach the hippocampus. Several experiments have emphasized the involvement of the LEC in episodic-like memory tasks such as object-place-context recognition[5,18,36] and odor-context associations,[21] where different pieces of information need to be combined. Nonetheless, there is still no conclusive evidence regarding the existence of entorhinal engrams, leaving this question partially unanswered. To assess the selective involvement of the EC in the OPCRT task, the product of the IEG *c-Fos* was utilized as an activity-dependent marker. The c-Fos marker has been extensively used in previous research to identify cell populations that are recruited during specific tasks and may undergo synaptic plasticity as a result of the experience.[37–40]

Mice subjected to the OPCRT task exhibited a higher number of c-Fos-positive cells in the LEC compared to mice that remained in their home cages. Notably, the difference between the two experimental groups was primarily observed in the

number of c-Fos-expressing cells rather than the individual cells' level of c-Fos protein fluorescence intensity. However, it should be noted that the relationship between fluorescence intensity and protein quantity in immunofluorescence staining is complex, making it difficult to rule out the possibility of differences in protein expression at the single-cell level, which may have been beyond the resolution of the technique we employed. Importantly, the increase in c-Fos cell density was specific to the LEC, as no significant increase in c-Fos expression was observed in either the MEC or the primary visual cortex (V1). These findings highlight the selective recruitment of the LEC during the OPCRT task. The *c-Fos* IEG has been widely employed to identify neuronal engrams, which are neuronal ensembles that become activated and undergo enduring changes in response to a specific experience or memory formation process, effectively serving as a memory trace.[41] Therefore, one possible interpretation of these results is that the selective increase in c-Fos within an LEC neuronal ensemble after the OPCRT task may indicate the presence of an episodic-like memory neuronal engram that encodes information about the experience over time.

Alternatively, the selective recruitment of the LEC observed in this study may reflect its role in processing local cues within the environment during the ongoing experience, without directly implicating it in memory processing. Previous research by Kuruvilla et al.[42] demonstrated that the LEC is responsible for processing local features, whereas the MEC is involved in processing global features of the environment. In the current study, the behavioral apparatus allowed animals to experience local cues such as visual patterns on the arena walls, objects, boundaries, and corners of the arena. However, global cues were absent because the arena was isolated from the surrounding room using a divider placed on top of the arena. Therefore, the specific recruitment of the LEC, rather than the MEC, may be attributed to the presence of local cues and the absence of global cues in the experimental setup. However, it is important to note that the processing of contextual information during the ongoing experience and the memory storage hypothesis are not mutually exclusive. It is plausible that the same LEC neurons recruited by the local features of the environment during the experience may also be involved in acquiring and storing that information for longer periods. One key characteristic of episodic-like memory is the automatic association of an event's memory with the context in which it occurs. Remarkably, LEC neurons have been shown to be crucial in contextualizing items, such as odors or objects, and are significantly modulated by specific combinations of items, places, and contexts during the ongoing experience.[5,6,16–18,21] This associative capability has also been observed in the hippocampus, a region where the existence of episodic-like memory engrams has been extensively demonstrated. Thus, the LEC emerges as an ideal candidate region not only for the processing of episodes but also for the immediate encoding and storage of new episodic memories. The processing of a new episodic-like memory-induced reversible long-term changes in LEC synaptic plasticity. The mechanisms underlying the persistent storage and retrieval of memories at the neurobiological level are still not fully understood. However, it is widely believed that strengthened synaptic connectivity between neurons involved in memory formation plays a crucial role in facilitating the reactivation of a group of neurons, known as engram cells, during memory recall.[43–46] The results revealed an occlusion of LTP in the superficial layers of the LEC 12 h after the execution of the OPCRT task, which was associated with enhanced LTD and increased basal synaptic transmission compared to the control and CNTX groups. These long-lasting modifications were reversible and followed the same time course of the OPCRT memory expression. We are aware that the observed synaptic modifications may not solely stem from c-Fos-expressing neurons. It is increasingly recognized that distinct engram populations, each serving unique functions, may be associated with the expression of different IEGs.[47] Consequently, the subset of LEC neurons affected by episodic-like memory processing and contributing to the observed synaptic plasticity effects with electrophysiology may extend beyond those expressing c-Fos. However, single-cell recordings in LEC layer II learning-tagged neurons confirmed a significant increase in synaptic strength. These results suggest that the acquisition of a new episodic-like memory can change the threshold for synaptic modification in the LEC circuit, at least within the superficial layers, similarly to what has been previously demonstrated in the lateral amygdala following fear conditioning[48,49] and in the neocortex after learning a motor task.[31] One possible explanation for these results is that enhanced synaptic transmission within the LEC circuitry may be crucial for reactivating the engram ensemble in the presence of natural recall cues, allowing for successful memory recall. However, when these plasticity changes return to baseline, the natural recall cues may not be as effective in reactivating the memory trace, resulting in the loss of episodic-like memory expression at the behavioral level. It is plausible to hypothesize that long-lasting forms of plasticity serve as a mechanism for recruiting the engram, considering that this episodic-like memory has a relatively short duration of a maximum of 12 h. However, it is important to note that the presence of such plasticity changes following memory tasks does not directly establish their role in memory storage and recall, as they could potentially contribute to other functions.[50] Here we show that the chemogenetic activation of LEC learning-tagged neurons is necessary and sufficient for the recall of episodic-like memories but not for non-associative memories. Moreover, the same neuronal ensemble is also naturally reactivated in response to recall cues. Comparing the reactivation of learning-tagged neurons during the test trial between mice capable of remembering associations and those that were not, a significant increase in ensemble reactivation was observed in the former group. Notably, reactivation levels exceeded chance levels, indicating that a substantial portion of the engram was reactivated even when the memory was not behaviorally expressed. However, this level of reactivation may not be sufficient for successful memory recall.

In conclusion, this work demonstrates the recruitment of the LEC during the OPCRT. The LEC is involved in the initial acquisition of episodic-like memories within the OPCRT paradigm, indicating its contribution to integrating various sensory cues, contextual details, and, potentially, even temporal information. This integration process is fundamental for creating coherent and meaningful memory representations. The activation of the LEC during the OPCRT supports the idea that it is specifically

engaged in the early stages of memory encoding, where the binding of different elements of an experience occurs.

Limitations of the study

While itis true that including both male and female mice could provide valuable insights into potential sex differences in episodic memory formation and recall, the primary objective of our research was to characterize the specific role of the EC in episodic memory and to demonstrate the existence of neuronal assemblies in this region displaying engram-like features. We opted to use male mice to reduce the potential confounding variables related to the use of female mice, such as hormonal fluctuation.

It is also essential to underline that chemogenetic and optogenetic techniques have limitations in replicating the natural patterns of neural activity during experiences and recall, as the inactivation and activation they induce are artificial.[51] Moreover, further investigations are necessary to characterize the cell types and the intrinsic circuits within the LEC involved in episodic-like memory recall. Existing evidence suggests that a specific subpopulation of superficial layer cells in the LEC, known as fan cells, plays a crucial role in the acquisition of episodic-like memory.[6] Therefore, it can be speculated that fan cells are part of the LEC engram ensemble. Nevertheless, the precise composition of the engram remains unknown. Exploring how different functional populations of LEC cells converge and coordinate to define an episode would be an intriguing direction for future research.

RESOURCE AVAILABILITY

Lead contact

Further information and requests for resources and reagents should be directed to the lead contact, Nicola Origlia (origlia@in.cnr.it).

Materials availability

This study did not generate new unique reagents.

Data and code availability

- All data reported in the main text or supplemental information are available from the lead contact upon request.
- All original code has been deposited at Zenodo and is publicly available as of the date of publication. The DOI is listed in the key resources table. All original code is also available from the lead contact upon request.
- Any additional information required to reanalyze the data reported in this paper is available from the lead contact upon request.

ACKNOWLEDGMENTS

We thank Nicoletta Berardi for helpful discussions. We also thank Renzo Di Renzo for technical assistance and Francesca Biondi for the excellent animal care. This work was supported by the Ministry of University and Research-PNRR project no. (THE) ECS_00000017 (A.C. and N.O.) and CNR project NutrAge (no. DSB.AD005.225).

AUTHOR CONTRIBUTIONS

F.T., methodology, data acquisition, data analysis, data curation, writing, editing, and figure production; S.G. and C.P., data acquisition and data curation; M.C.v.d.O., production of the AAV packaged as serotype 5 virus and editing; M.M. and A.C., conceptualization, writing, and editing; N.O., project management, funding acquisition, methodology, data analysis, data curation, writing, editing, and figure production.

DECLARATION OF INTERESTS

The authors declare no competing interests.

STAR★METHODS

Detailed methods are provided in the online version of this paper and include the following:

- KEY RESOURCES TABLE
- EXPERIMENTAL MODEL AND SUBJECT DETAILS
- METHOD DETAILS
  - AAV vectors and stereotaxic injections
  - Behavioral apparatus
  - 4-Hydroxytamoxifen treatment
  - Chemogenetic intervention
  - Immunohistochemistry
  - In-vitro electrophysiology
- QUANTIFICATION AND STATISTICAL ANALYSIS

SUPPLEMENTAL INFORMATION

Supplemental information can be found online at https://doi.org/10.1016/j.celrep.2024.114795.

Received: December 22, 2023
Revised: July 16, 2024
Accepted: September 9, 2024

REFERENCES

1. Griffiths, D., Dickinson, A., and Clayton, N. (1999). Episodic memory: what can animals remember about their past? Trends Cogn. Sci. *3*, 74–80.
2. Eacott, M.J., and Norman, G. (2004). Integrated memory for object, place, and context in rats: a possible model of episodic-like memory? J. Neurosci. *24*, 1948–1953.
3. Eacott, M.J., Easton, A., and Zinkivskay, A. (2005). Recollection in an episodic-like memory task in the rat. Learn. Mem. *12*, 221–223.
4. Easton, A., Zinkivskay, A., and Eacott, M.J. (2009). Recollection is impaired, but familiarity remains intact in rats with lesions of the fornix. Hippocampus *19*, 837–843.
5. Wilson, D.I.G., Watanabe, S., Milner, H., and Ainge, J.A. (2013). Lateral entorhinal cortex is necessary for associative but not nonassociative recognition memory. Hippocampus *23*, 1280–1290.
6. Vandrey, B., Garden, D.L.F., Ambrozova, V., McClure, C., Nolan, M.F., and Ainge, J.A. (2020). Fan Cells in Layer 2 of the Lateral Entorhinal Cortex Are Critical for Episodic-like Memory. Curr. Biol. *30*, 169–175.e5.
7. Aggleton, J.P., Wright, N.F., Rosene, D.L., and Saunders, R.C. (2015). Complementary Patterns of Direct Amygdala and Hippocampal Projections to the Macaque Prefrontal Cortex. Cereb. Cortex *25*, 4351–4373.
8. Nadel, L., and Moscovitch, M. (1998). Hippocampal contributions to cortical plasticity. Neuropharmacology *37*, 431–439.
9. Nadel, L., and Peterson, M.A. (2013). The hippocampus: part of an interactive posterior representational system spanning perceptual and memorial systems. J. Exp. Psychol. Gen. *142*, 1242–1254.
10. Ranganath, C., and Ritchey, M. (2012). Two cortical systems for memory-guided behaviour. Nat. Rev. Neurosci. *13*, 713–726.
11. Rugg, M.D., and Vilberg, K.L. (2013). Brain networks underlying episodic memory retrieval. Curr. Opin. Neurobiol. *23*, 255–260.

12. Dickerson, B.C., and Eichenbaum, H. (2010). The episodic memory system: neurocircuitry and disorders. Neuropsychopharmacology *35*, 86–104.
13. Wang, C., Chen, X., Lee, H., Deshmukh, S.S., Yoganarasimha, D., Savelli, F., and Knierim, J.J. (2018). Egocentric coding of external items in the lateral entorhinal cortex. Science *362*, 945–949.
14. Bowler, J.C., and Losonczy, A. (2023). Direct cortical inputs to hippocampal area CA1 transmit complementary signals for goal-directed navigation. Neuron *111*, 4071–4085.e6.
15. Lee, J.Y., Jun, H., Soma, S., Nakazono, T., Shiraiwa, K., Dasgupta, A., Nakagawa, T., Xie, J.L., Chavez, J., Romo, R., et al. (2021). Dopamine facilitates associative memory encoding in the entorhinal cortex. Nature *598*, 321–326.
16. Burwell, R.D. (2000). The parahippocampal region: corticocortical connectivity. Ann. N. Y. Acad. Sci. *911*, 25–42.
17. Hargreaves, E.L., Rao, G., Lee, I., and Knierim, J.J. (2005). Major dissociation between medial and lateral entorhinal input to dorsal hippocampus. Science *308*, 1792–1794.
18. Wilson, D.I.G., Langston, R.F., Schlesiger, M.I., Wagner, M., Watanabe, S., and Ainge, J.A. (2013). Lateral entorhinal cortex is critical for novel object-context recognition. Hippocampus *23*, 352–366.
19. Tsao, A., Moser, M.-B., and Moser, E.I. (2013). Traces of experience in the lateral entorhinal cortex. Curr. Biol. *23*, 399–405.
20. Qasim, S.E., Miller, J., Inman, C.S., Gross, R.E., Willie, J.T., Lega, B., Lin, J.-J., Sharan, A., Wu, C., Sperling, M.R., et al. (2019). Memory retrieval modulates spatial tuning of single neurons in the human entorhinal cortex. Nat. Neurosci. *22*, 2078–2086.
21. Persson, B.M., Ambrozova, V., Duncan, S., Wood, E.R., O'Connor, A.R., and Ainge, J.A. (2022). Lateral entorhinal cortex lesions impair odor-context associative memory in male rats. J. Neurosci. Res. *100*, 1030–1046.
22. Umbach, G., Kantak, P., Jacobs, J., Kahana, M., Pfeiffer, B.E., Sperling, M., and Lega, B. (2020). Time cells in the human hippocampus and entorhinal cortex support episodic memory. Proc. Natl. Acad. Sci. USA *117*, 28463–28474.
23. Tsao, A., Sugar, J., Lu, L., Wang, C., Knierim, J.J., Moser, M.-B., and Moser, E.I. (2018). Integrating time from experience in the lateral entorhinal cortex. Nature *561*, 57–62.
24. Bright, I.M., Meister, M.L.R., Cruzado, N.A., Tiganj, Z., Buffalo, E.A., and Howard, M.W. (2020). A temporal record of the past with a spectrum of time constants in the monkey entorhinal cortex. Proc. Natl. Acad. Sci. USA *117*, 20274–20283.
25. Bellmund, J.L., Deuker, L., and Doeller, C.F. (2019). Mapping sequence structure in the human lateral entorhinal cortex. Elife *8*, e45333.
26. Montchal, M.E., Reagh, Z.M., and Yassa, M.A. (2019). Precise temporal memories are supported by the lateral entorhinal cortex in humans. Nat. Neurosci. *22*, 284–288.
27. Choi, J.-H., Sim, S.-E., Kim, J.-I., Choi, D.I., Oh, J., Ye, S., Lee, J., Kim, T., Ko, H.-G., Lim, C.-S., and Kaang, B.K. (2018). Interregional synaptic maps among engram cells underlie memory formation. Science *360*, 430–435.
28. Roy, D.S., Park, Y.-G., Kim, M.E., Zhang, Y., Ogawa, S.K., DiNapoli, N., Gu, X., Cho, J.H., Choi, H., Kamentsky, L., et al. (2022). Brain-wide mapping reveals that engrams for a single memory are distributed across multiple brain regions. Nat. Commun. *13*, 1799.
29. Matos, M.R., Visser, E., Kramvis, I., van der Loo, R.J., Gebuis, T., Zalm, R., Rao-Ruiz, P., Mansvelder, H.D., Smit, A.B., and van den Oever, M.C. (2019). Memory strength gates the involvement of a CREB-dependent cortical fear engram in remote memory. Nat. Commun. *10*, 2315.
30. Guenthner, C.J., Miyamichi, K., Yang, H.H., Heller, H.C., and Luo, L. (2013). Permanent genetic access to transiently active neurons via TRAP: targeted recombination in active populations. Neuron *78*, 773–784.
31. Rioult-Pedotti, M.S., Friedman, D., and Donoghue, J.P. (2000). Learning-induced LTP in neocortex. Science *290*, 533–536.
32. Fyhn, M., Molden, S., Witter, M.P., Moser, E.I., and Moser, M.-B. (2004). Spatial representation in the entorhinal cortex. Science *305*, 1258–1264.
33. Hafting, T., Fyhn, M., Molden, S., Moser, M.-B., and Moser, E.I. (2005). Microstructure of a spatial map in the entorhinal cortex. Nature *436*, 801–806.
34. Doan, T.P., Lagartos-Donate, M.J., Nilssen, E.S., Ohara, S., and Witter, M.P. (2019). Convergent Projections from Perirhinal and Postrhinal Cortices Suggest a Multisensory Nature of Lateral, but Not Medial, Entorhinal Cortex. Cell Rep. *29*, 617–627.e7.
35. Nilssen, E.S., Doan, T.P., Nigro, M.J., Ohara, S., and Witter, M.P. (2019). Neurons and networks in the entorhinal cortex: A reappraisal of the lateral and medial entorhinal subdivisions mediating parallel cortical pathways. Hippocampus *29*, 1238–1254.
36. Criscuolo, C., Fontebasso, V., Middei, S., Stazi, M., Ammassari-Teule, M., Yan, S.S., and Origlia, N. (2017). Entorhinal Cortex dysfunction can be rescued by inhibition of microglial RAGE in an Alzheimer's disease mouse model. Sci. Rep. *7*, 42370.
37. Guzowski, J.F., McNaughton, B.L., Barnes, C.A., and Worley, P.F. (1999). Environment-specific expression of the immediate-early gene Arc in hippocampal neuronal ensembles. Nat. Neurosci. *2*, 1120–1124.
38. Barth, A.L., Gerkin, R.C., and Dean, K.L. (2004). Alteration of neuronal firing properties after in vivo experience in a FosGFP transgenic mouse. J. Neurosci. *24*, 6466–6475.
39. Smeyne, R.J., Schilling, K., Robertson, L., Luk, D., Oberdick, J., Curran, T., and Morgan, J.I. (1992). fos-lacZ transgenic mice: mapping sites of gene induction in the central nervous system. Neuron *8*, 13–23.
40. Wang, K.H., Majewska, A., Schummers, J., Farley, B., Hu, C., Sur, M., and Tonegawa, S. (2006). In vivo two-photon imaging reveals a role of arc in enhancing orientation specificity in visual cortex. Cell *126*, 389–402.
41. Ramirez, S., Liu, X., Lin, P.-A., Suh, J., Pignatelli, M., Redondo, R.L., Ryan, T.J., and Tonegawa, S. (2013). Creating a false memory in the hippocampus. Science *341*, 387–391.
42. Kuruvilla, M.V., and Ainge, J.A. (2017). Lateral Entorhinal Cortex Lesions Impair Local Spatial Frameworks. Front. Syst. Neurosci. *11*, 30.
43. McKernan, M.G., and Shinnick-Gallagher, P. (1997). Fear conditioning induces a lasting potentiation of synaptic currents in vitro. Nature *390*, 607–611.
44. Rogan, M.T., Stäubli, U.V., and LeDoux, J.E. (1997). Fear conditioning induces associative long-term potentiation in the amygdala. Nature *390*, 604–607.
45. Tye, K.M., Prakash, R., Kim, S.-Y., Fenno, L.E., Grosenick, L., Zarabi, H., Thompson, K.R., Gradinaru, V., Ramakrishnan, C., and Deisseroth, K. (2011). Amygdala circuitry mediating reversible and bidirectional control of anxiety. Nature *471*, 358–362.
46. Nabavi, S., Fox, R., Proulx, C.D., Lin, J.Y., Tsien, R.Y., and Malinow, R. (2014). Engineering a memory with LTD and LTP. Nature *511*, 348–352.
47. Sun, X., Bernstein, M.J., Meng, M., Rao, S., Sørensen, A.T., Yao, L., Zhang, X., Anikeeva, P.O., and Lin, Y. (2020). Functionally Distinct Neuronal Ensembles within the Memory Engram. Cell *181*, 410–423.e17.
48. Hong, I., Kim, J., Lee, J., Park, S., Song, B., Kim, J., An, B., Park, K., Lee, H.W., Lee, S., et al. (2011). Reversible Plasticity of Fear Memory-Encoding Amygdala Synaptic Circuits Even after Fear Memory Consolidation. PLoS One *6*, e24260.
49. Tsvetkov, E., Carlezon, W.A., Benes, F.M., Kandel, E.R., and Bolshakov, V.Y. (2002). Fear conditioning occludes LTP-induced presynaptic enhancement of synaptic transmission in the cortical pathway to the lateral amygdala. Neuron *34*, 289–300.
50. Dringenberg, H.C. (2020). The history of long-term potentiation as a memory mechanism: Controversies, confirmation, and some lessons to remember. Hippocampus *30*, 987–1012.
51. Belzung, C., Turiault, M., and Griebel, G. (2014). Optogenetics to study the circuits of fear- and depression-like behaviors: A critical analysis. Pharmacol. Biochem. Behav. *122*, 144–157.

52. Schneider, C.A., Rasband, W.S., and Eliceiri, K.W. (2012). NIH Image to ImageJ: 25 years of image analysis. Nat. Methods *9*, 671–675.

53. Cicconet, M., and Hochbaum, D.R. (2019). A Supervised, Symmetry-Driven, GUI Toolkit for Mouse Brain Stack Registration and Plane Assignment. bioRxiv. https://doi.org/10.1101/781880.

54. Lueptow, L.M. (2017). Novel Object Recognition Test for the Investigation of Learning and Memory in Mice. J. Vis. Exp. *126*, 55718. https://doi.org/10.3791/55718.

55. Mathis, A., Mamidanna, P., Cury, K.M., Abe, T., Murthy, V.N., Mathis, M.W., and Bethge, M. (2018). DeepLabCut: markerless pose estimation of user-defined body parts with deep learning. Nat. Neurosci. *21*, 1281–1289.

56. Origlia, N., Righi, M., Capsoni, S., Cattaneo, A., Fang, F., Stern, D.M., Chen, J.X., Schmidt, A.M., Arancio, O., Yan, S.D., and Domenici, L. (2008). Receptor for advanced glycation end product-dependent activation of p38 mitogen-activated protein kinase contributes to amyloid-beta-mediated cortical synaptic dysfunction. J. Neurosci. *28*, 3521–3530.

57. Origlia, N., Bonadonna, C., Rosellini, A., Leznik, E., Arancio, O., Yan, S.S., and Domenici, L. (2010). Microglial receptor for advanced glycation end product-dependent signal pathway drives beta-amyloid-induced synaptic depression and long-term depression impairment in entorhinal cortex. J. Neurosci. *30*, 11414–11425.

58. Gabrielli, M., Prada, I., Joshi, P., Falcicchia, C., D'Arrigo, G., Rutigliano, G., Battocchio, E., Zenatelli, R., Tozzi, F., Radeghieri, A., et al. (2022). Microglial large extracellular vesicles propagate early synaptic dysfunction in Alzheimer's disease. Brain *145*, 2849–2868. https://doi.org/10.1093/brain/awac083.

STAR★METHODS

KEY RESOURCES TABLE

REAGENT or RESOURCE	SOURCE	IDENTIFIER
Antibodies		
Rabbit monoclonal anti-cFos	Synaptic Systems	cat# 226 008; RRID: AB_2891278
Rat monoclonal anti-mCherry	ThermoFisher Scientific	cat# M11217; RRID: AB_2536611
Donkey polyclonal anti-Rabbit Alexa Fluor 488	Jackson Immunoresearch	cat. no. 711-545-152; RRID: AB_2313584
Goat polyclonal anti-Rat Alexa Fluor 568	Jackson Immunoresearch	cat# A11077; RRID:AB_2534121
Bacterial and virus strains		
AAV-Fos:CreER^{T2}	Matos et al.[29]	N/A
AAV1/2-hSyn1:DIO-hM3Dq-mCherry	UZH-VVF	v89-1
AAV5/2-hSyn1:DIO-hM4Di-mCherry	UZH-VVF	v84-5
AAV1/2-hSyn1:DIO-mCherry	UZH-VVF	v116-1
Chemicals, peptides, and recombinant proteins		
4-Hydroxytamoxifen	Sigma-Aldrich	H6278
Clozapine N-oxide hydrochloride	Merck	cat. no. 34233-7
Experimental models: organisms/strains		
Mouse: C57BL/6J	Charles River	N/A
Software and algorithms		
Python version 3.8	Python Software Foundation	https://www.python.org/
MATLAB	MathWorks	https://kr.mathworks.com/
Prism 8	GraphPad	https://www.graphpad.com/
ImageJ	Schneider et al.[52]	https://imagej.net/
Cell counting algorithm	Cicconet et al.[53]	https://www.biorxiv.org/content/10.1101/781880v1
Behavioral classifier algorithm	Custom code Tozzi F.	Zenodo: https://doi.org/10.5281/zenodo.13369258

EXPERIMENTAL MODEL AND SUBJECT DETAILS

All experimental procedures involving animals followed the guidelines defined by the European legislation (Directive 2010/63/EU), and the Italian Legislation (LD no. 26/2014). The Organism Responsible for Animal Welfare (OPBA) of the National Research Council of Italy (CNR) Institute of Neuroscience in Pisa and the Italian Ministry of Health approved the study protocol (authorization n. 16/2022-PR).

Male wild-type C57BL/6J mice were housed in conventional cages (365 × 207 × 140 mm, 2–3 animals per cage) with nesting material on a 12-h light/dark cycle with food and water available *ad libitum*. Behavioral experiments were performed on 3-month-old male mice during the light phase and mice were randomly assigned to experimental groups. To control for order and cage effects, each cage contained a mixture of mice from the experimental and control groups.

METHOD DETAILS

AAV vectors and stereotaxic injections

AAV-FosCreERT2 (titer: 1.2×10^{13}) and Cre-dependent AAVs AAV-hSynDIO-hM3Dq-mCherry, AAV-hSynDIO-hM4Di-mCherry and AAV-hSynDIO-mCherry (titers: $5.0–6.0\times10^{12}$) were packaged as serotype 5 virus. The AAV-FosCreERT2 vector was obtained from Matos et al.,[29] while the Cre-dependent AAVs AAV-hSynDIO-hM3Dq-mCherry, AAV-hSynDIO-hM4Di-mCherry, and AAV-hSynDIO-mCherry vectors were purchased from the UZH viral vector facility (Zurich, Switzerland).

For stereotaxic injections, 2-month-old male C57BL/6J mice were deeply anesthetized using an intraperitoneal injection of Zoletil 100 (zolazepam and tiletamine, 1:1, 40 mg/kg; Laboratoire Virbac) and Xilor (xilazine 2%, 10 mg/kg; Bio98). After the tail pinch reflex disappearance, mice were positioned in the stereotaxic apparatus. Lidocaine (2%) was topically applied to the skull to provide local analgesia. The scalp was shaved and a midline incision was made. A bilateral craniotomy was performed at the stereotaxic coordinates targeting the LEC (AP -4.0 mm, ML ± 4.0 mm from bregma, measured on the skull surface). A glass pipette was lowered from the brain's surface at an 11° angle until a slight bend in the pipette indicated contact with the dura as described by Vandrey et al.[6] The

pipette was retracted 0.1 mm and 125 nL of a virus mixture of AAV-FosCreERT2 and Cre-dependent AAV (ratio 1:500, AAV-FosCreERT2 at a final titer of 2.4×10^{10}) was injected. Then, the pipette was retracted again by 0.1 mm and an additional 125 nL of the virus mixture was injected, for a total of 250 nL. This approach minimized the likelihood of the spread of the virus into adjacent cortical structures. For all injections, the pipette was slowly retracted after a stationary period of 5 min. Then, the scalp was sutured and the mouse was brought back to its cage for recovery. Animals remained in their home cage for 3 weeks until the start of behavioral experiments.

Behavioral apparatus

The test environment was composed of two square boxes (length 40 cm, width 40 cm, height 40 cm) with different visual cues on the walls to provide distinct contexts. Context A had gray walls and context B had four different visual cues on the four walls: black and white vertical stripes, black triangles on a white background, black and white horizontal stripes, and black circles on a white background. The wall and floor of the environment were cleaned with 30% alcohol before each trial. Objects were household items of approximately the same size as the mouse and varying in color, shape, and texture. To avoid odor cues, new identical copies of each object were used for each trial, and objects were cleaned with 30% alcohol after each trial.

Behavioral tasks

For the behavioral tests, 3-month-old C57BL/6J mice were habituated to the experimenter by extensive handling for one week before the experiments. The performance of specific tasks that included the novel location test (NLT) and the novel object-place-context recognition test (OPCRT) was always preceded by the open field test to control locomotion and anxious behavior in the same arena used for behavioral testing.

During the behavioral tasks, object exploration was monitored via an overhead camera. For all sample and test trials, mice were allowed to explore the environment freely for 3 min. If the animals did not meet the minimum exploration time of 20 s for both objects, the scoring was continued past 3 min for a maximum of 10 min until total exploration reached 20 s.[54] Between the two sample trials, mice were removed to a holding cage for approximately 1 min while the next environment was configured for the subsequent trial. The test trial was instead performed either 1 h, 6 h, 12 h, or 48 h after the sample trials presentation for the OPCRT, and 12 h for the NLT. For each task, the novel object at the test, the context, and the quadrants where the novel object or configuration occurred were counterbalanced across animals and experimental conditions.

Open field. Before the execution of the memory tasks, mice were allowed to explore for 5 min the same context in which they were given the same trial of the subsequent behavioral test. A custom-made Python pipeline was used to automatically compute the total ambulatory distance as well as the amount of time spent in the outer zones versus inner zones (24 cm × 24 cm).

Novel location test. During the sample trials, mice were exposed to two copies of an object in a given context. Then, the mice were removed from the box and brought back into their home cages for 12h before the presentation of the test trial. In the test trial, one of the two objects was moved to a novel location (novel location) while the other was kept in the same location as the sample trial (familiar location) and the context remained the same.

Novel object-place-context recognition test. In the OPCRT, in the first sample trial mice were presented with two different novel objects in context A or B. After the first sample trial, mice were removed from the box and placed in a holding cage for a 1-min inter-trial interval (i.t.i.) while the box was cleaned. In the second sample trial, mice were presented with the same objects in opposite locations in different contexts. In the test trial, mice were presented with two copies of one of the objects within the same context used in the first sample trial. At the test, one copy of the object is in a novel location for the test context (novel OPC configuration), whereas the other copy is in a familiar location for the test context (familiar OPC configuration). As a behavioral control (without novelty) a different group of mice(OCT group) explored two identical objects in context A or B. In the second sample trial, after a 1-min inter-trial interval, mice were presented with the same pair of objects in the same positions but in a different context. In the test trial, mice were presented with the same pair of objects from the sample trials in the context used in the first sample trial.

Contexts exposure. As a control in electrophysiology experiments, mice of the CNTX group were allowed to explore a sequence of A-B-A or B-A-B empty contexts for 5 min each. Between each context exploration, mice were removed from the box and placed in a holding cage for 1-min i.t.i., while the box was cleaned.

Animal tracking. Behavioral videos were recorded using an AUKEY webcam 1080p full HD camera and were then analyzed offline. Different mouse body regions, namely the nose, the two ears, the back of the animal, the middle portion, and the tip of the tail labeled using the open-source tool DeepLabCut[55] for markerless pose estimation. For this purpose, 460 frames extracted from 23 videos were manually labeled and used to train the DeepLabCut ResNet50 network for 103000 iterations, obtaining a high-fidelity tracking of the selected body parts. The animal tracking allowed to automate of the calculation of the animal speed, the total traveled distances, and the time spent in different regions of the arena (center/periphery) in the open field test, the novel location test, and in the novel object-place-context recognition test. Moreover, the tracking results were also used to automatically calculate the discrimination index of the animals during the memory test by combining pose estimation with a machine learning algorithm.

Behavioral scoring. In order to obtain a reproducible and efficient scoring of the behavioral tests, a random forest classifier was trained to discriminate between epochs of object exploration and epochs of no exploration by using the distances of the tracked body parts from the two objects (custom code available at Zenodo: https://doi.org/10.5281/zenodo.13369258). This approach

allowed us to automatically detect the time spent by the animal exploring either the novel or the familiar object and calculate the corresponding discrimination index. To train the classifier, 156414 frames from 16 videos were manually labeled as "exploration" or "no exploration", the results of the classifier were compared with the traditional scoring using a stopwatch and the frame-by-frame manual scoring as the ground truth.

To determine the relative exploration of novel and familiar configurations, the time spent exploring the familiar and novel objects was converted into a discrimination index (DI) according to the formula:

$$DI = T_{Novel} - T_{familiar} / T_{Novel} + T_{familiar}$$

4-Hydroxytamoxifen treatment

4OH-TAM (H6278, Sigma-Aldrich) was injected into an aqueous solution. A 50 mg/mL stock of 4OH-TAM in DMSO (D8418, Sigma-Aldrich) was realized and maintained at −20°C. On the day of the experiment, a final solution of 4OH-TAM 2.5 mg/mL was obtained in two steps: first, diluting the stock solution 1:10 in saline containing 2% Tween80 (P1754, Sigma-Aldrich) and then adding a volume of saline. The final solution contained 2.5 mg/mL of 4OH-TAM, 5% DMSO, and 1% Tween80 in saline. Mice received 4OH-TAM (25 mg per Kg, i.p.) 4h before the sample trials.[29] To reduce the stress from i.p. injections, mice were anesthetized shortly using isofluorane (3%) and were injected while unconscious.

Chemogenetic intervention

Clozapine N-oxide hydrochloride (CNO; cat. no. 34233–7, Merck) was dissolved in sterile saline. For behavioral experiments, mice received 3 mg per kg (i.p.) CNO 30 min before each test session.

Immunohistochemistry

Mice were deeply anesthetized using urethane (Merck, 20% solution, 0.1 mL/100 g body weight) and perfused with an intracardiac infusion with PBS pH 7.4, followed by 4% paraformaldehyde (PFA) in PBS pH 7.4. Brains were removed, post-fixed for 24h in 4% PFA (w/vol) solution, and then immersed in 30% sucrose (w/vol) in PBS. Brains were then sliced into 50 μm coronal sections using a freezing microtome (Leica) and free-floating sections were processed for immunofluorescence.

The cortical sections were incubated for 2h in a blocking solution at 22°C–24°C containing 5% BSA (w/vol) and 0.5% Triton X-100 (v/v) in PBS, and incubated overnight at 4°C with anti-cFos monoclonal antibody (cat. no. 226 008, Synaptic Systems) diluted 1:1000 and anti-mCherry monoclonal antibody (cat. no. M11217, ThermoFisher Scientific) diluted 1:1000 in PBS with 1% BSA (w/vol) and 0.1% Triton X-100 (v/v). Sections were then washed with PBS and incubated for 2h at 22°C–24°C with Alexa Fluor 488-conjugated secondary antibody (cat. no. 711-545-152, Jackson Immunoresearch) and Alexa Fluor 568-conjugated secondary antibody (cat. no. A11077, ThermoFisher Scientific) added at a dilution of 1:300 in the same solution as the primary antibody. Sections were then washed 3 times with PBS and mounted on slides, then they were air-dried and coverslipped with FluoromountTM aqueous mounting medium (cat. no. F4680, Merck). Imaging was performed on an Axio Imager Z2 microscope (Carl Zeiss) and multichannel images were produced with ApoTome 2 using an EC Plan-NEOFLUAR 10x/0.3 objective. Images were processed using ImageJ (NIH, USA) to split channels, adjust brightness/contrast, and perform z-projection (maximum intensity).

cFos and mCherry quantification

The cFos+ cell detection was performed using a modified version of the puncta-detecting algorithm described in Cicconet et al.[53] followed by manual refinement of the detection results. Several parameters in the pipeline were optimized to process the experimental brain slices. To detect individual cFos+ nuclei via Laplacian of Gaussian filtering of the image, the local maxima that corresponded to cfos puncta were found and distinguished from the local maxima in the background. For the analysis, the software parameters were set to: background threshold: 10, sigma: 3.5, and circularity threshold:0.3. The detection results were then supervised by an operator and eventually modified to correct for inaccuracies. The density of cFos+ cells (cFos+/mm2) was averaged over 6–10 sections per animal. For the mCherry+ cell detection, cell counting was manually performed by an operator blind to the experimental conditions, when possible, and the mCherry+ cell density (mCherry+/mm2) was averaged over 4–6 sections per animal. The LEC and MEC regions of interest (ROIs) were manually outlined, using ImageJ, based on the mouse brain atlas (Paxinos and Franklin's The Mouse Brain in Stereotaxic Coordinates).

To analyze the overlap between cFos and mCherry-expressing cells, the percentage of overlap was calculated as the number of cFos+, mCherry+ double-positive cells divided by the average number of dapi+ cells. The chance level of overlap was calculated as the product between the number of cFos+ positive and mCherry+ cells, divided by the average number of dapi+ cells. The average number of dapi+ cells was obtained by averaging the number of dapi+ nuclei in 6–9 LEC sections obtained from 7 animals.

In-vitro electrophysiology

Electrophysiology was performed as in Origlia et al.,.[56] Mice were anesthetized with urethane i.p. injections (20% sol (w/vol), 0.1 mL/100 g of body weight) and decapitated. Horizontal EC-hippocampal slices (400 μm of thickness) were produced using a vibratome (Leica VT1200S). All steps were performed in ice-cold oxygenated artificial cerebrospinal fluid (ACSF) containing the

following (in mM): 119 NaCl, 2 CaCl2, 1.2 MgSO4, 1 NaH2PO4, 6.2 NaHCO3, 10 HEPES, 11 glucose. Slices were then transferred to a chamber and perfused at a 2–3 mL/min rate. Field excitatory postsynaptic potentials (fEPSPs) were evoked by a concentric bipolar stimulating electrode and recorded in the II/III layers of EC.

Basal recordings were carried out using stimulus intensity evoking a response whose amplitude was 50–60% of the maximal amplitude. After 10 min of stable baseline, long-term potentiation (LTP) or long-term depression (LTD) was induced using either high-frequency stimulation (HFS, three trains of 100 pulses at 100 Hz, 10 s interval) or low-frequency stimulation (LFS, 900 paired pulses at 1 Hz, the interval between paired pulses was 30 ms). After HFS or LFS, fEPSPs were monitored every 20 s for at least 60 min or 40 min respectively. The magnitude of LTP or LTD was calculated as the average of the relative amplitudes (compared to baseline) of fEPSPs recorded in the last 10 min. Values were expressed as percentage changes relative to the baseline. Whole cell patch-clamp recordings were performed as previously described[57,58] on visually identified EC layer II neurons. Cells were visualized under DIC illumination, using a 63× immersion objective (Zeiss). A multiclamp 700A amplifier (Molecular Devices) and a 1550B Digidata (Molecular Devices) were used to acquire electrophysiological recordings with pClamp 10.7 software (Molecular Devices). Holding potential was set at − 70 mV for spontaneous excitatory postsynaptic currents recording (see Figure S2).

QUANTIFICATION AND STATISTICAL ANALYSIS

All data are reported as mean ± SEM. Statistical analysis was performed with GraphPad Prism 8 software (GraphPad Software, San Diego, CA). The Shapiro–Wilk test for normality was used to determine if the data were normally distributed. For electrophysiological experiments statistical comparisons between experimental groups were performed by applying a two-way repeated-measures ANOVA with pairwise multiple comparison procedure (Holm-Sidak method, unless otherwise stated). For behavioral experiments, a one-way ANOVA or an unpaired t test were applied to determine differences in average discrimination indices and exploration rates between groups. One-sample t test was used to determine whether the average discrimination index for each group was different from chance (hypothesized mean = 0). A two-way ANOVA was applied for the evaluation of differences in c-fos cell density or single-cell mean fluorescence intensity. Kruskal-Wallis was used to determine differences in the discrimination indices among different time points in the analysis of the time course of episodic-like memory. All of the statistical details of experiments can be found in the figure legends.